CHIRALITY 21:S153–S162 (2009)

Molecular and Supramolecular Chirality in Gemini-Tartrate Amphiphiles Studied by Electronic and Vibrational Circular Dichroisms

AURÉLIE BRIZARD,[1] DAMIEN BERTHIER,[1] CAROLE AIMÉ,[1] THIERRY BUFFETEAU,[2]*
DOMINIQUE CAVAGNAT,[2] LAURENT DUCASSE,[2] IVAN HUC,[1] AND REIKO ODA[1]*

[1]*Institut Européen de Chimie et Biologie (IECB), Université de Bordeaux (CNRS UMR5248), Pessac Cedex 33607, France*
[2]*Institut des Sciences Moléculaires, Université de Bordeaux (CNRS UMR5255), Talence Cedex 33405, France*

Contribution to the Special Thematic Project "Advances in Chiroptical Methods"

ABSTRACT This contribution presents an application of electronic circular dichroism (ECD) and vibrational circular dichroism (VCD) to study the molecular and supramolecular chirality in assemblies of gemini-tartrate amphiphiles. Nonchiral dicationic *n*-2-*n* amphiphiles (n = 14–20) can self-organize into right- or left-handed structures upon interacting with chiral tartrate counterions. Micellar solutions can also be obtained for shorter alkyl chains (n = 12). First, the conformation of tartrate counterions has been investigated in various environments (micellar solutions and chiral ribbons). ECD and VCD spectra recorded in micellar solutions are independent from the solvent and from the nature of the cations (sodium, cetyl-trimethylammonium, or dimeric surfactant 12-2-12) used and are representative of the anticonformation of the tartrate dianions. On the other hand, drastic changes in the ECD and VCD spectra have been observed in multilayered chiral assemblies of 16-2-16 tartrate. These strong spectral modifications are associated with the chiral arrangement of the tartrate molecules at the surface of the bilayers. Moreover, chirality transfer from counterions to achiral amphiphiles has been clearly evidenced by VCD since circular dichroism has been observed on vibrations related to alkyl chains and gemini headgroups. Finally, ECD and VCD experiments were performed varying the enantiomeric excess of the tartrate. The ECD and VCD intensities do not vary linearly with the enantiomeric excess of the anion and different behaviors have been observed from the two spectroscopic methods: ECD intensities are correlated to the pitch of the ribbons, whereas the VCD intensities are correlated to the dimension of the chiral ribbons. *Chirality 21:S153–S162, 2009.*

KEY WORDS: vibrational circular dichroism; supramolecular chirality; twisted membranes; gemini amphiphile; tartrate

INTRODUCTION

Chiral amphiphilic molecules often assemble in solution to form aggregates with high-aspect ratios, such as rods, tapes, or tubes.[1,2] Their morphology frequently expresses the chirality of their components at a supramolecular scale of nanometers to micrometers; the fibrous structures may be coiled, twisted, or wound around one another and exist as a left-handed or a right-handed form. On fundamental grounds, the relationship between molecular chirality (∼Å) and supramolecular chirality (∼μm) as expressed in these structures represents an excellent model for studying the emergence of specific shapes at a macroscopic scale through cooperative interaction between a large number of very small building blocks. In addition to this fundamental aspect, chiral fibrous objects possess a great potential for development of new functional supramolecular devices, taking advantage of the chirality of the molecular constituents organized in a hierarchical manner and/or of the supramolecular chirality of the fibers that can be generated.

We have previously reported that nonchiral cationic gemini surfactants having the formula C_sH_{2s}-1,2-$((CH_3)_2N^+C_nH_{2n+1})_2$, denoted as *n-s-n*, form twisted or helical ribbons in solution for $s = 2$ and $n \geq 14$ in the presence of chiral tartrate counterions.[3,4] These helical

Additional Supporting Information may be found in the online version of this article.

Contract grant sponsors: CNRS (Chemistry Department), Région Aquitaine.

*Correspondence to: T. Buffeteau, Institut des Sciences Moléculaires, Université de Bordeaux (CNRS UMR5255), 351 cours de la Libération, 33405 Talence Cedex, France. E-mail: t.buffeteau@ism.u-bordeaux1.fr or R. Oda, Institut Européen de Chimie et Biologie (IECB), Université de Bordeaux (CNRS UMR5248), 2 rue Robert Escarpit, 33607 Pessac Cedex, France. E-mai: r.oda@iecb.u-bordeaux.fr

Received for publication 11 May 2009; Accepted 4 August 2009
DOI: 10.1002/chir.20790
Published online 6 November 2009 in Wiley InterScience (www.interscience.wiley.com).

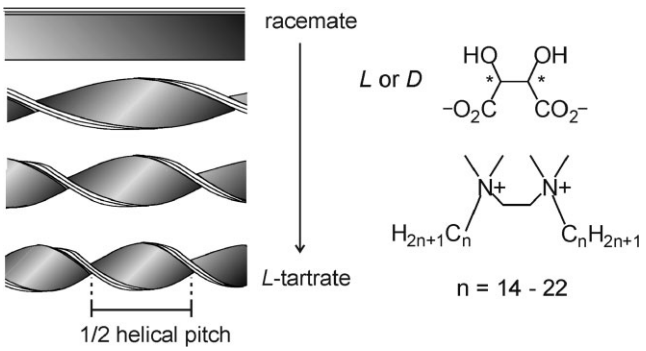

Fig. 1. Structure of *n*-2-*n* dicationic amphiphiles having tartrate counterions and schematic representation of the multi-bilayer twisted ribbons they form in water. The pitch of the ribbons can be tuned upon varying the enantiomeric excess of the anion.

fibers form continuous networks that gel some organic solvents as well as water.[3] Right-handed ribbons are formed in the presence of L-tartrate, and left-handed ribbons are formed with D-tartrate. The width and the pitch of the ribbons can be continuously tuned upon mixing the D- and L-enantiomers of tartrate in various proportions, from flat multilayer membranes for the racemate (infinite pitch) to the ribbons of the pure enantiomer (pitch is about 200 nm) as shown in Figure 1.[4] Chirality induction by the tartrates was shown to involve selective anion–cation recognition and conformationally labile chirality in the cations induced by interactions with the chiral anions.[5] Recently, a detailed molecular organization of the flat ribbons of the racemate and of the twisted or helical ribbons of the pure tartrate enantiomer has been proposed in the hydrated state from a multiscale approach involving small-angle and wide-angle X-ray scattering (SAXS and WAXS) and molecular modeling.[6] It has been shown that the three-dimensional molecular organizations of these structures include interdigitation of alkyl chains within each bilayer and well-defined networks of ionic and hydrogen bonds between cations, anions, and water molecules between bilayers. Each tartrate dianion adopts an anticonformation and lies flat at the bilayer surface between adjacent gemini headgroups and above the end of the alkyl chains belonging to the other leaflet. Tartrate molecules in the same monolayer are at the same height as the ammonium headgroups and are oriented parallel to each other. Water molecules seem to play a crucial role in bridging tartrates through hydrogen bonds. The high cohesion between the individual chiral units of the ribbon structure is likely at the origin of the expression of chirality at the scale of the entire ribbon.

Gemini-tartrate amphiphiles represent excellent models for studying molecular chirality of tartrate dianions in various environments. Indeed, dicationic amphiphiles with $n \geq 14$ form twisted or helical ribbons, whereas micelles are formed for $n = 12$ or when cetyl-trimethylammonium (CTA) replaces the dimeric surfactant. It is important to determine the conformation of tartrates in these two types of aggregates to understand the role of the chiral inducer in the self-assembled structures. Tartrate salts can, in principle, adopt three different conformations of the carbon chain, denoted T, G^+, and G^- (Fig. 2). The anticonformation (T) is the most commonly encountered in solution and in the solid state[7] but the interaction with a dicationic amphiphile may affect this predominant conformation. On the other hand, when tartrate molecules are confined in a helical structure, their molecular chirality will be interconnected to the supramolecular chirality of the helical ribbons. Consequently, the chiral contribution of the tartrate molecules is not only dependent on the tartrate conformation but also to their chiral arrangement at the bilayer surface. Conformational studies in such supramolecular systems are not straightforward and require spectroscopic methods for probing chirality at the molecular level.

One of the most versatile tools for studying assemblies of chiral molecules is electronic circular dichroism (ECD).[8,9] Because of its high sensitivity, this spectroscopic technique has been widely practiced to monitor the formation of helical superstructures and the formation of gels through self-assembly processes.[10] A number of useful correlations, rules, or procedures for relating the signs of the measured optical activity and absolute configuration have been established for a variety of structural motifs. Meanwhile, all such empirical methods suffer from exceptions that in some cases were preceded by incorrect assignments. Indeed, the assignment of CD bands to the transitions of the chromophores to which they are allied is not always direct because significant bathochromic or hypsochromic shifts may occur upon aggregation. Vibrational circular dichroism (VCD) may provide extra information compared with ECD in the UV/Visible range. VCD is an extension into the infrared (IR) region of the spectrum where vibrational transitions occur in the ground electronic state of a molecule. The method measures the differential absorption of left versus right circularly polarized IR radiation by a molecular vibration transition.[11,12] The advantage of VCD over ECD is the large amount of information for 3*N*-6 vibrations, where *N* is the number of atoms in the molecule. Another advantage is reliable theoretical support. Quantum mechanical predictions of VCD spectra are quite successful in replicating the corresponding experimental spectra in the mid-IR region.[13] Ab initio calculations combined with VCD experiments has been used during the two last decades to determine the absolute configuration of small and medium-sized molecules[12–14] and more recently to elucidate supramolecular structures.[15–24] Moreover, several VCD studies of dialkyl tartrates (essentially dimethyl-tartrate) have been performed to determine their predominant conformation in various solvents (CCl_4, DMSO-d_6 CS_2, D_2O),[25–28] complexed with cyclodextrins[28] and confined in lecithin reverse micelles.[29]

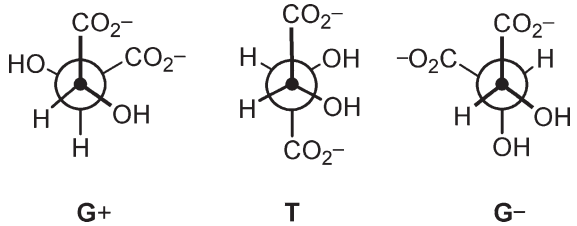

Fig. 2. Main three conformers of L-tartrate.

In the present contribution, ECD and VCD have been used to characterize the molecular and supramolecular chirality in gemini-tartrate amphiphiles. Molecular chirality of tartrate molecules has been studied in micellar solution (CTA-tartrate or 12-2-12 tartrate), whereas supramolecular chirality has been evidenced in multilayered assemblies of 16-2-16 tartrate. Finally, the relation between the chiroptical properties of the self-organized systems and the structural parameters of the ribbons (pitch, width, and thickness) has been revealed by varying the enantiomeric excess of the anion.

MATERIALS AND METHODS

Materials

The 16-2-16 amphiphile with bromide counterions were synthesized as previously reported.[30] The procedure for bromide to tartrate exchange was modified as follows from the initially reported use of DOWEX resin.[3] A suspension of the silver salt of the tartaric acid in deionized water (MilliQ) was prepared freshly before each use upon mixing D- or L-tartaric acid and Ag_2CO_3 (0.5 equiv), followed by vigorous stirring under slight vacuum for 1 h. A solution of the 16-2-16 surfactant (stoichiometric amount, typically 500 mg to 2 g scale) was added, and the mixture was stirred for 5 min and lyophilized. The resulting powder was dissolved in methanol and filtered on Celite to give a colorless solution. After evaporation, the product was dissolved in a mixture of chloroform/methanol (9/1, v/v), precipitated upon addition of ethyl acetate, filtered, and then dried. The high yield of ion exchange and the stoichiometry were confirmed by element analysis.

UV/Vis and CD Measurements

UV/Vis absorption and circular dichroism measurements were performed on a Varian Cary 300 UV–Vis spectrometer and a Jobin-Yvon CD6-SPEX circular dichrograph, respectively. Quartz cuvettes with optical path lengths of 2 mm (absorption) and 1 mm (CD) were used. The spectra were measured for 10 mM solutions or gels.

IR and VCD Measurements

The infrared and VCD spectra were recorded with a ThermoNicolet Nexus 670 FTIR spectrometer equipped with a VCD optical bench.[31] In this optical bench, the light beam was focused on the sample by a BaF_2 lens (191 mm focal length), passing an optical filter (depending on the studied spectral range), a BaF_2 wire grid polarizer (Specac), and a ZnSe photoelastic modulator (Hinds Instruments, Type II/ZS50). The light was then focused by a ZnSe lens (38.1 mm focal length) onto a 1×1 mm^2 HgCdTe (ThermoNicolet, MCTA* E6032) detector. IR absorption and VCD spectra were recorded at a resolution of 4 cm^{-1}, by coadding 50 scans and 24,000 scans (8 h acquisition time), respectively. Experiments in D_2O were performed at a concentration of 100 mM using a cell assembled from CaF_2 windows and a 50 μm Teflon spacer. Experiments in $CHCl_3$ were performed at a concentration of 20 mM in a variable path length cell (250 μm) with BaF_2 windows. For gel samples, a solution heated with a hair dryer were held in the cell. The gel is obtained by letting the system go at room temperature. Each experiment has been reproduced five times to obtain reliable results. Since the filling of the cell may induce molecular orientation in confined medium for self-assembled systems, vibrational linear dichroism spectra were systematically measured before each VCD experiment.* Baseline corrections of the VCD spectra were performed by subtracting the raw VCD spectra of the solvent. The photoelastic modulator was adjusted for a maximum efficiency in the mid-IR region at 1600 cm^{-1} in D_2O solvent and 1300 cm^{-1} in $CHCl_3$ solvent (3000 cm^{-1} for experiments in the CH stretching region). Calculations were performed via the standard ThermoNicolet software, using Happ and Genzel apodization, de-Haseth phase-correction and a zero-filling factor of one. Calibration spectra were recorded using a birefringent plate (CdSe) and a second BaF_2 wire grid polarizer, following the experimental procedure previously published.[32] Finally, in the presented absorption spectra, the solvent absorption was subtracted out.

RESULTS AND DISCUSSION

Conformation of Tartrates in Solution and in Micellar Aggregates

The main conformation of tartrate salts has been evaluated using electronic circular dichroism (ECD) in the absorption region of the carboxylate chromophores, at 190–250 nm, as shown in Figure 3. In aqueous solution, the ECD spectrum of sodium L-tartrate is temperature independent and shows two negative bands at 194 and 211 nm (Fig. 3A). The latter band is due to the n-π^* transition of the carboxylate group. This transition is forbidden and appears as a shoulder (at 209 nm) in the UV spectrum. The absence of exciton coupling between the carboxylates is consistent with the expected T conformation, in which the transition moments of the two chromophores are coplanar and remote from each other, two factors that decrease coupling. Similar ECD spectra were observed when sodium is replaced by cetyl-trimethylammonium (CTA) or dimeric surfactant 12-2-12, two cationic amphiphiles forming micellar aggregates.

The absorption and VCD spectra of sodium L-tartrate in D_2O solution and of CTA and 12-2-12 tartrate micelles dispersed in D_2O are shown in Figure 4. Because of the interference from D_2O absorption, IR and VCD spectra can only be measured in the 1800–1250 cm^{-1} region. This spectral region is characterized by the strong antisymmetric ($\nu_a CO_2^-$) and symmetric ($\nu_s CO_2^-$) stretching modes of the carboxylate groups of the tartrate at 1602 and 1392

*The vibrational linear dichroism (VLD) spectra were recorded using the same spectrometer and external accessory bench. For these experiments, the PEM modulated the polarization of the infrared beam between the parallel and perpendicular linear polarization states with respect to a reference direction, and the demodulation of the polarization modulated signal with the lock-in amplifier was performed at 2fm =100 kHz. VLD spectra were recorded for two cell orientations (rotated by 45°) in the plane perpendicular to the beam propagation. If no VLD bands were observed in the mid-infrared region for the two cell orientations, the sample may be considered as an isotropic medium and VCD experiments can be performed.

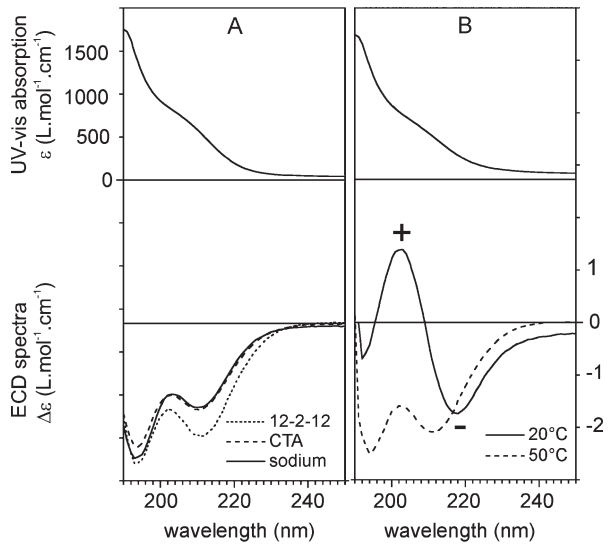

Fig. 3. UV–Vis absorption (top) and ECD (bottom) spectra of carbonyl chromophores of L-tartaric acid derivatives in H_2O at room temperature. (**A**) Absorption spectrum of sodium L-tartrate and CD spectra of sodium L-tartrate, CTA L-tartrate, and 12-2-12 L-tartrate. (**B**) Absorption spectrum of 16-2-16 L-tartrate and its CD spectra at 20°C and 50°C.

cm^{-1}, respectively; by the bending modes of methyl ($\delta_a CH_3$, $\delta_{s'} CH_3$ and $\delta_s CH_3$) and methylene (δCH_2) groups of the amphiphilic cations in the 1490–1410 cm^{-1} region; and by the bending mode of the C*H of the tartrate at 1342 cm^{-1}.[33] The VCD spectrum of sodium L-tartrate solution exhibit a negative couplet (positive at higher frequency and negative at lower frequency) for the $\nu_a CO_2^-$ mode, whereas no bands are observed for the $\nu_s CO_2^-$ mode. On the basis of the degenerate coupled-oscillator (DCO) model (particularly well adapted to interpret the VCD spectra of dimeric molecules),[34,35] this non observation of VCD bands is consistent with the T conformation in which the transition moments of the two $\nu_s CO_2^-$ modes are coplanar. No changes are observed in the VCD spectra of L-tartrate in micellar aggregates, indicating that the anti-conformation of tartrate is not modified when sodium is replaced by CTA or 12-2-12 dimeric surfactant. Polavarapu et al. have shown that the C*—O stretching vibrations can be also used to determine the conformation of tartaric acid and its esters.[26] The C*—O stretching vibrations are expected in the 1130–1050 cm^{-1} region and have been found insensitive to intermolecular interactions. To observe these bands, we have recorded IR and VCD spectra of CTA L- and D-tartrate micelles dispersed in $CHCl_3$ solvent (Fig. 5).

In $CHCl_3$ solvent, the absorption spectrum can be obtained in the 1800–1250 and 1190–950 cm^{-1} regions. The antisymmetric and symmetric stretching vibrations of the carboxylate groups of the tartrate are located at 1610 and 1351 cm^{-1}, respectively. The $\nu_a CO_2^-$ mode is observed at higher frequency than that observed in D_2O solution, whereas the $\nu_s CO_2^-$ mode is found at lower frequency. These frequency shifts are essentially due to hydrogen-bonding effects which are present in D_2O solution and have been observed in the carbonyl stretching region of dimethyl-tartrate.[28] The IR band associated with the $\nu_s CO_2^-$ mode exhibits a dissymmetrical shape because it contains contributions of the bending modes of OH and C*H of the tartrate. The IR bands located at 1114 and 1053 cm^{-1} can be assigned to the symmetric and antisymmetric combinations of C*—O stretching motions, respectively. The high splitting in frequency of the two modes (~60 cm^{-1}) indicates a strong coupling of the associated oscillators. Considering the DCO model, a negative couplet is expected in the VCD spectrum of L-tartrate for the T conformation displaying a 60° counterclockwise dihedral angle of the O—C*—C*—O segment, whereas a positive couplet is expected for the G^- conformation.[26] It is noteworthy that no VCD bands are assumed for the G^+ conformation since the two C*—O groups are coplanar.

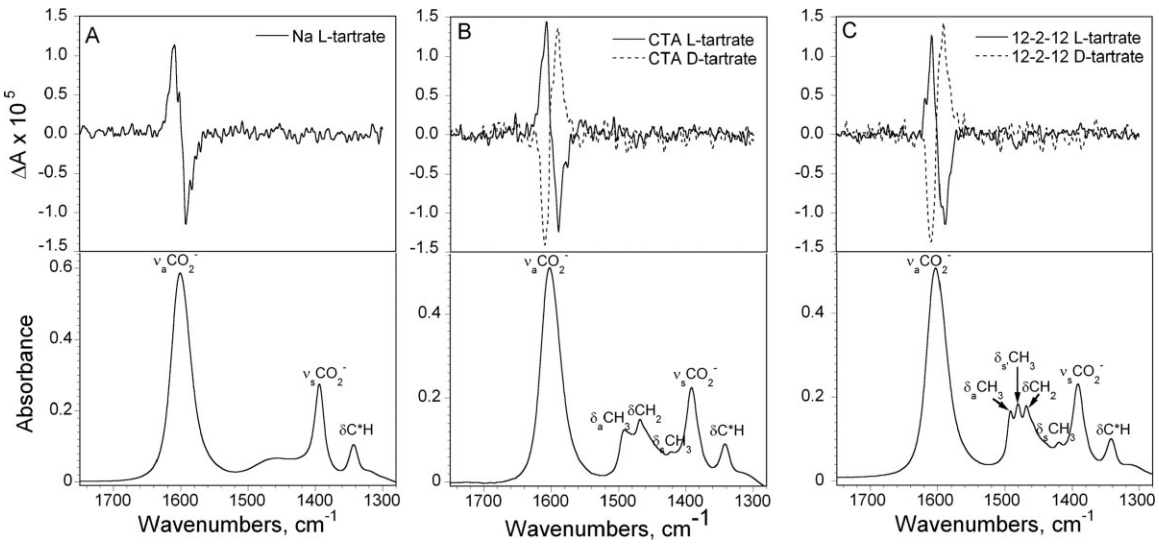

Fig. 4. VCD (top) and IR (bottom) spectra of (**A**) sodium L-tartrate, (**B**) CTA L- and D-tartrate, and (**C**) 12-2-12 L- and D-tartrate, recorded at 100 mM in D_2O at room temperature with a path length of 50 μm.

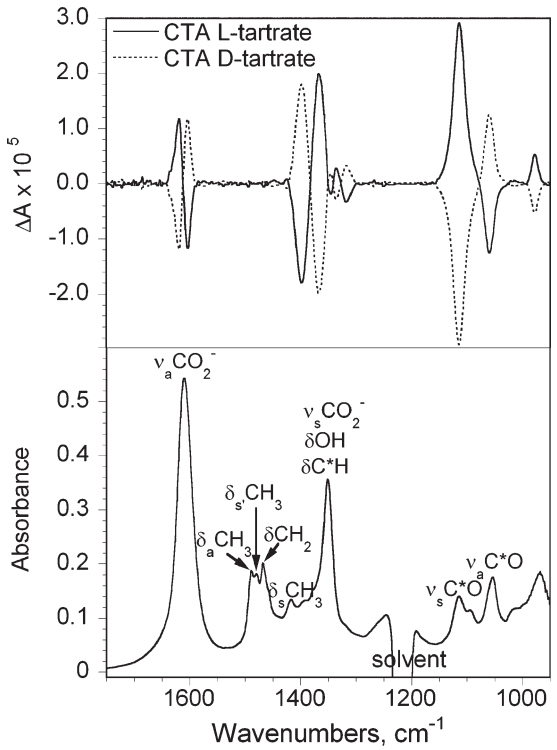

Fig. 5. VCD (top) and IR (bottom) spectra CTA L- and D-tartrate, recorded at 20 mM in $CHCl_3$ at room temperature with a path length of 250 μm.

The VCD spectrum of CTA L-tartrate micelles dispersed in $CHCl_3$ solution exhibit a negative C*—O stretching couplet in the 1170–1010 cm^{-1} region. This couplet is distinctly biased to positive intensity at 1114 cm^{-1}, as previously observed in the VCD spectra of dimethyl-L-tartrate in CCl_4 solution.[26–28] The shape as well as the intensity of this couplet were perfectly reproduced by ab initio calculations, confirming the anticonformation of dimethyl-L-tartrate.[27,28] Thus, the observed VCD associated with the C*—O stretching vibrations can be interpreted in favor to the anticonformation of tartrate. Finally, a negative couplet is also observed for the $\nu_a CO_2^-$ mode (the intensity is similar to that observed in D_2O solution), whereas a positive couplet appeared in the 1430–1330 cm^{-1} region. The latter couplet is associated with OH bending vibrations.

On the basis of the ECD and VCD observations, we can conclude that tartrate salts show a strong preference for the T conformation, presumably as a result of the charge repulsions. This anticonformation is independent on the solvent (D_2O, $CHCl_3$) and the cation (sodium, CTA, 12-2-12) used.

Conformation of Tartrates in Twisted Ribbons

As shown in Figure 3B, the ECD spectrum of L-tartrate is completely different when sodium is replaced by 16-2-16 amphiphile which assembles into chiral bilayer. A strong negative exciton coupling between the carboxylates is then observed at 20°C, with a positive peak at 202 nm and a negative peak at 219 nm. The zero of the exciton band at 209 nm matches with a maximum (shoulder) in the absorption spectrum. Such negative exciton coupling suggests, in a first qualitative analysis, a counterclockwise arrangement of the electric transition moments, as found in G^- conformation. However, in the present case, the tartrate molecules are organized in a chiral arrangement to form submicrometric chiral aggregates and the ECD spectrum should include this supramolecular chirality. Therefore, from ECD spectra only, it is very difficult to discriminate the two types of chirality (molecular and supramolecular) and to give their respective contribution on the ECD spectrum. Finally, when the bilayers are heated at 50°C above their melting temperature, a reversible transition from bilayer toward spherical micelles is observed, and the ECD spectrum is similar to that observed for the 12-2-12 dimeric surfactant.

The VCD spectra of tartrates in twisted ribbons also reveal strong differences with those obtained for micellar aggregates. The VCD spectrum of membranes of 16-2-16 L-tartrate (Fig. 6) features a bisignate band for the $\nu_a CO_2^-$ mode, but the band is much more intense (by a factor 6) and its sign is opposite to that of the band of CTA L-tartrate. The spectrum also shows a weaker negative band for the $\nu_s CO_2^-$ mode which is not seen in the spectrum of CTA L-tartrate. As mentioned for ECD experiments, a conformational change of tartrate ions upon forming twisted membranes could explain these spectral modifications at a first sight. However, examination of the VCD spectrum in the C*—O stretching vibration region observed for 16-2-16 tartrate twisted ribbons in $CHCl_3$ shows that greatest care must be taken in the interpretation of these spectral modifications. Indeed, a negative couplet (positive band for the symmetric combinations of C*—O stretching motions at 1114 cm^{-1} and negative band for the antisymmetric combinations of C*—O stretching motions at 1063 cm^{-1}) is observed in this spectral region. As mentioned earlier, considering the exciton coupling theory, a negative couplet is expected for the T conformation of L-tartrates whereas a positive couplet is expected for the G^- conformation. Therefore, the negative couplet observed in the C*—O stretching vibration region for twisted ribbons of 16-2-16 tartrate is not consistent with the G^- conformation of tartrate assuming that the exciton coupling originates from intramolecular conformation but rather suggests that even in the twisted ribbons, L-tartrates remain with T conformation. This result certainly indicates that the important changes in the ECD and VCD spectra as well as the enhancement of the VCD intensity observed in these self-assembled systems are governed by the chiral intermolecular arrangement of the tartrate ions in the membranes. This is in agreement with our recent data by X-ray diffraction experiments associated with molecular modeling showing that tartrate dianions adopt an anticonformation at the chiral bilayer surface.[6]

Induction of Chiral Conformations in the Cationic Amphiphile

In the UV–Vis region, *n*-2-*n* amphiphiles have no chromophores that could indicate chiral induction measurable

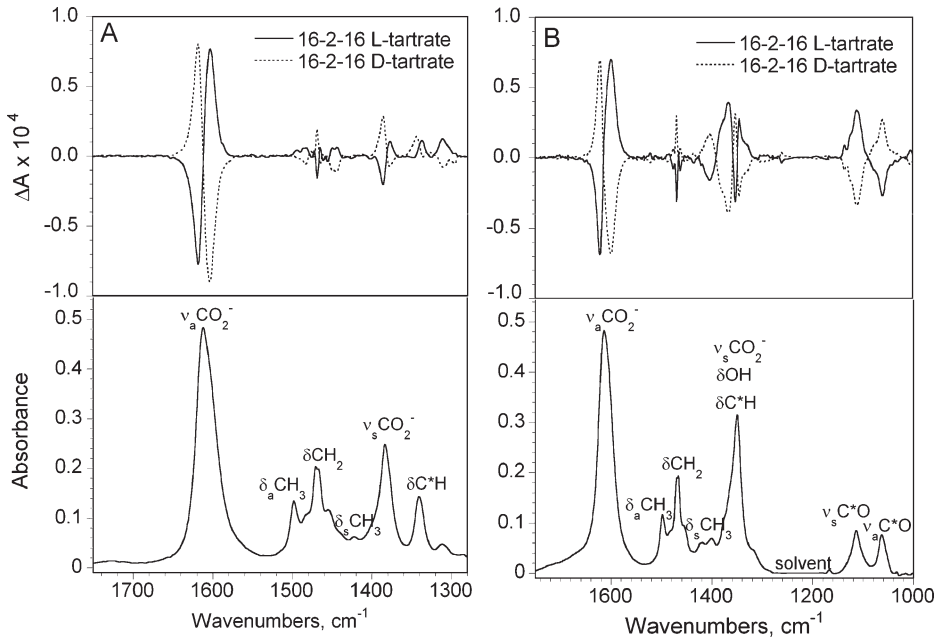

Fig. 6. VCD (top) and IR (bottom) spectra of **(A)** 16-2-16 L- and D-tartrate recorded at room temperature at 100 mM in D_2O with a path length of 50 μm and **(B)** at 20 mM in $CHCl_3$ with a path length of 250 μm.

by ECD experiments. On the contrary, a direct observation of the chiral induction can be obtained by vibrational circular dichroism measurements, since in the infrared region vibrators belonging to tartrate dianions and the amphiphilic cations can be easily distinguished. Thus, as shown in Figure 6, the VCD spectra of membranes of 16-2-16 L-tartrate in D_2O and $CHCl_3$ feature a negative and a weak positive bands for the two split components of the bending mode of methylene groups (δCH_2) located at 1470 and 1466 cm^{-1}, respectively. Two bands exhibiting opposite signs are found in the VCD spectrum of the D-tartrate derivative, showing that this is not an artifact from the noise of the spectrum. Since tartrate ions do not absorb in this region (Fig. 4A), it can be concluded that this band belongs to the cationic amphiphile and is induced by the tartrate anions.

To confirm this result, we have recorded the VCD spectra of the same samples in the 3000–2800 cm^{-1} region associated with the antisymmetric (ν_aCH_2) and symmetric (ν_sCH_2) stretching vibrations of the methylene groups. As shown in Figure 7A, the VCD spectra of 16-2-16 L- or D-tartrate counterions reveal very intense induced bands both for the ν_aCH_2 mode at 2918 cm^{-1} and for the ν_sCH_2 mode at 2850 cm^{-1}. The frequencies obtained for the ν_aCH_2 and ν_sCH_2 modes along with the δCH_2 mode which shows a splitting indicate that the alkyl chains are well organized in an orthogonal packing with mainly an all trans conformation. For micellar solutions (Fig. 7B), the stretching vibrations of methylene groups are observed at higher frequencies (2925 and 2854 cm^{-1} for the ν_aCH_2 and ν_sCH_2 modes, respectively) and the splitting of the δCH_2 band disappears, indicating the presence of many gauche conformations and disordered chains. The VCD spectrum of CTA tartrate micelles do not reveal induced bands in the CH_2 stretching region. Only a weak VCD band is observed at 2928 cm^{-1} assigned to the C*H stretching vibration of tartrate dianions.[33] Since similar VCD spectra have been obtained for 12-2-12 L-tartrate, no chiral induction from the anion to the cation takes place in micelles when cations and anions are poorly associated. Thus, the chiral induction only takes place in membranes when cations and anions cooperatively organize in a multilayer structure.

Effect of Enantiomeric Excess on Chiroptical Properties

Pure 16-2-16 L-tartrate forms right-handed helical ribbons, whereas the D-enantiomer forms ribbons of opposite handedness. Transmission electron microscopy (TEM) observations show that when mixed in various proportions, the two enantiomers mix homogeneously and form twisted ribbons with a continuous variation of twist pitch, width, and thickness.[4] Thus, an increase of the enantiomeric excess (ee) causes a decrease of the twist pitch from infinite (flat ribbons) to 200 nm (pure enantiomer) as well as a decrease of the width (from 200 nm to 25 nm) and the thickness of the ribbons. Various gels were prepared in H_2O (for ECD experiments) or in D_2O (for VCD experiments) by mixing the two pure enantiomers to follow the dependence of the ECD and VCD intensities on ee.

The ECD spectra of various mixtures of the two enantiomers of 16-2-16 tartrate are reported in Figure 8A. ee = 1 corresponds to the pure 16-2-16 D-tartrate gel. While a decrease of the enantiomeric excess causes a decrease of the intensity of the positive exciton coupling between the carboxylates, regardless the value of ee, a positive exciton coupling is observed, indicating a similar chiral environment of the tartrate dianions. A linear dependence could be expected if a complete phase separation of the enan-

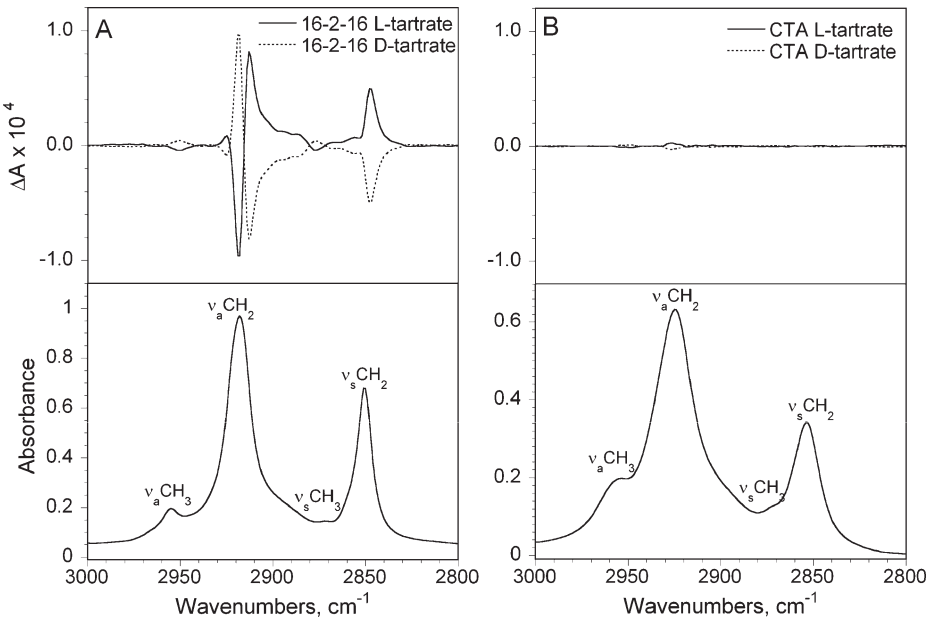

Fig. 7. VCD (top) and IR (bottom) spectra of (**A**) 16-2-16 L- and D-tartrate and (**B**) CTA L- and D-tartrate, recorded at 100 mM in D_2O at room temperature with a path length of 50 μm.

tiomers into twisted ribbons of opposite handedness occurs or if the two enantiomers forms flat ribbons and the ECD intensity arises from the excess 16-2-16 D-tartrate enantiomer. In the present case, TEM images show no phase separation or flat ribbons for enantiomeric excess ranging between 0.2 and 0.8. A continuous evolution of the ribbon morphology has been evidenced (change of the twist pitch) with a handedness of the ribbons given by the enantiomer in excess. As is shown in Figure 8B, a nonlinear dependence of the ECD intensity with ee is observed. It is noteworthy that the ECD intensity show a very good correlation with the inverse of the pitch period as observed with TEM images, a parameter which is directly related to the supramolecular chirality. This result suggests again that the ECD intensities reproduce not only the variation of the molecular chirality but also the emergence of a supramolecular chirality.

The VCD spectra of various mixtures of the two enantiomers of 16-2-16 tartrate are reported in the spectral ranges associated with the tartrate dianions (Fig. 9A) and the cations (Fig. 9B). For all the value of the enantiomeric excess, intense VCD bands are observed both for carboxylate vibrations (tartrate dianions) and for the CH_2 stretching vibrations of the aliphatic chains (gemini cations). This reveals again a chiral arrangement of the tartrate dianions, but more interestingly a chiral induction in the membranes. However, strikingly, unlike the dependence of the ECD intensity on ee, VCD intensities increase when the enantiomeric excess decrease and reach a maximum for ee close to 0, before rapidly going down to 0 when ee is strictly equal to 0. The lower the molecular chirality is, the higher the VCD intensities. This unexpected behavior cannot be simply explained by a supramolecular chirality (the pitch of the chiral ribbons) since the decrease of the enantiomeric excess is associated with the formation of increasingly flat ribbons (decreasing chirality). Therefore, the variation of the pitch period of the twisted ribbons cannot be at the origin of the observed effects.

However, the pitch period of the twisted ribbons is not the only supramolecular parameter that varies with ee. The width and the thickness (or number of bilayers) of the ribbons formed by 16-2-16 tartrate are also affected by a modification of ee. We have observed that the mean width of ribbons decreases from 200 nm to 25 nm with an increase of the enantiomeric excess from 0 to 1. As for the thickness of the ribbons, it is directly linked to the number of bilayers (nb) inside the ribbons. We have also reported in Ref. 6 that the ribbons formed with 16-2-16 tartrate follow strict molecular organization and are made of stacked heterochiral bilayers comprised of homochiral monolayers, and this organization is conserved through large morphology transitions from racemic (i.e., flat multilayered ribbons) to chiral ribbons as well as tubules of the pure enantiomer. The chirality of mono/bilayers are defined not only by the molecular chirality of tartrate (D- or L-) but also by gemini dications which are intrinsically achiral but can adopt two mirror-image conformations of their headgroups, noted or (i.e.,). The contact domain between adjacent bilayers is homochiral: both gemini headgroups and tartrate of the symmetrical leaflet have the same chirality (Fig. S1 in Supporting Information). In the racemate, the infinite alternation of domains between bilayers having and arrays of headgroups and tartrate ions is possible without chirality frustration. In contrast, if

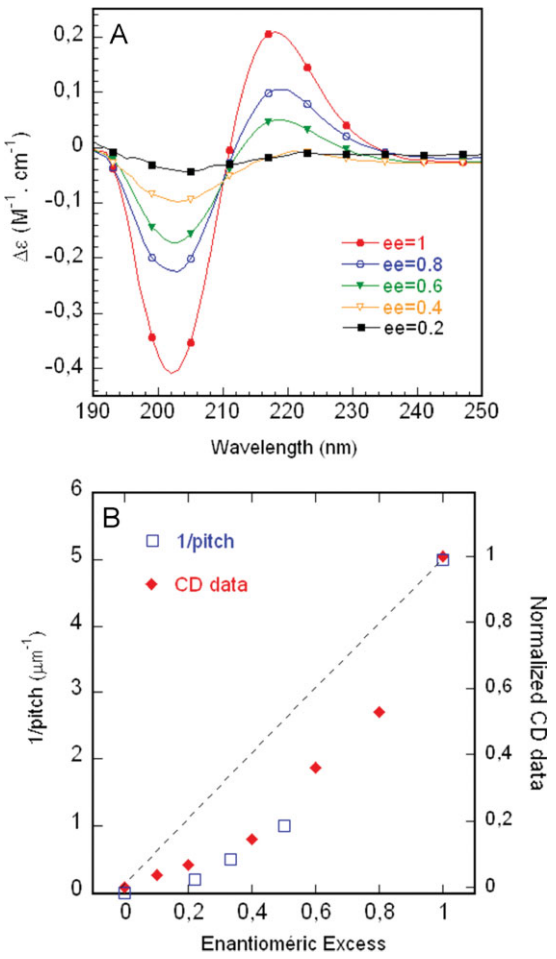

Fig. 8. (**A**) ECD spectra of various mixtures of the two enantiomers of 16-2-16 tartrate recorded at room temperature at 10 mM in H_2O with a path length of 1 mm. (**B**) Variation of the inverse of the pitch period (left) and the normalized CD data (right) as a function of enantiomeric excess. [Color figure can be viewed in the online issue, which is available at www.interscience.wiley.com.]

we follow this rule, in the case of a pure enantiomer (L for instance), only two bilayers can stack, separated by a domain with an array of headgroups and tartrate ions. In the external leaflets of these double-bilayer ribbons, the heterochiral bilayer packing requires that the gemini conformation is , and obviously, the only available tartrate (L) cannot be accommodated within the chiral cavity where D-tartrates are expected. From this rule, the number of bilayers of the ribbons can be expected to follow the relationship: nb = 2/ee. The ribbon thickness estimated from TEM images, in spite of large polydispersity especially at low ee, confirms this tendency (Fig. 10A). The ribbon thickness is very close to (2/ee) × 3.25 nm as obtained from X-ray powder diffraction.

This stacking of bilayers suggests that while the tartrate counterions adopts a crystal-like organization at the inner surfaces of the two bilayers, those of the outer surfaces are much more loosely organized (Fig. S1 in Supporting Information) reminiscent of micellar surfaces. Such a difference between the organization of inner and outer tartrate may explain in part the enhancement of the VCD signal when ee decreases. Indeed, as nb increases with the decrease of ee, the ratio $R_{\text{outside/inside}}$ of outside gemini-tartrate vs. inside gemini-tartrate decrease with the following relationship: $R_{\text{outside/inside}} = 1/(\text{nb} - 1)$. For ee = 1 this ratio is 1, whereas for ee = 0.2 it is 1/9. Therefore, the effect of loosely organized gemini-tartrate becomes negligible for low ee. The variation of the width of the ribbons is an other explanation of the enhancement of the VCD signal since it is also linked to the ratio of loose vs. crystalline organization of gemini-tartrate through the edge effect of the bilayers. As illustrated in Figure S1 of Supporting Information, lower the ee, larger the ribbons, and smaller the ratio of loosely linked gemini-tartrate with respect to those with crystalline organization. On the other hand, it is important to note that the contribution of "free" tartrate and gemini dications in solution by exchange with those in the ribbons is negligible. Indeed, the cmc of 16-2-16 tartrate is less than 10^{-6} mol/l whereas ECD and VCD experiments were performed at 10 mM and 100 mM, respectively.

The increase of the VCD intensity when the ee decreases seems to be therefore related to the increase of the size of the chiral ribbons as well as to a better molecular arrangement of the cationic amphiphiles. Indeed, the evolution of the normalized intensities of the antisymmetric stretching vibrations of the carboxylate and methylene groups are correlated to the thickness (Fig. 10A) and the width (Fig. 10B) of the twisted ribbons. Thus, since all chiral molecules, regardless of their D- or L- absolute configuration, are involved in ribbons that overall possesses the same macroscopic handedness (dictated by the enantiomer in excess), a larger number of molecules involved in the larger and thicker ribbons may be at the origin of the enhancement of the VCD intensity. Moreover, a better arrangement of both the tartrate dianions and the cationic amphiphiles is certainly obtained for larger pitch period (lower ee) since the curvature of the membrane is less important and the ratio of molecules involved in the edge of ribbons with nonorganized manner is smaller. Nevertheless, at very low enantiomeric excess (ee < 0.1), VCD intensity decreases and tends toward a zero value as expected.

This behavior clearly shows that VCD intensities in self-organized systems are very dependent on the size and the molecular organization of the investigated objects. This effect is well observed in VCD experiments since the wavelength in the infrared region is significantly higher than the size of the twisted ribbons. This structural parameter must be taken into account to interpret correctly VCD spectra. A similar behavior has been already observed, though not as dramatic as the one reported here, in VCD experiments on polypeptide samples having different molecular weights.[31,36] The intensity of the VCD couplet (positive couplet for poly-γ-benzyl-L-glutamate[31] and negative couplet for poly-L-lysine at pH ~7[36]) in the amide I region increases monotonously with the molecular weight of the polypeptides. For poly-L-lysine, this feature has been interpreted by an increase in stability for a specific conformation of left-handed helical

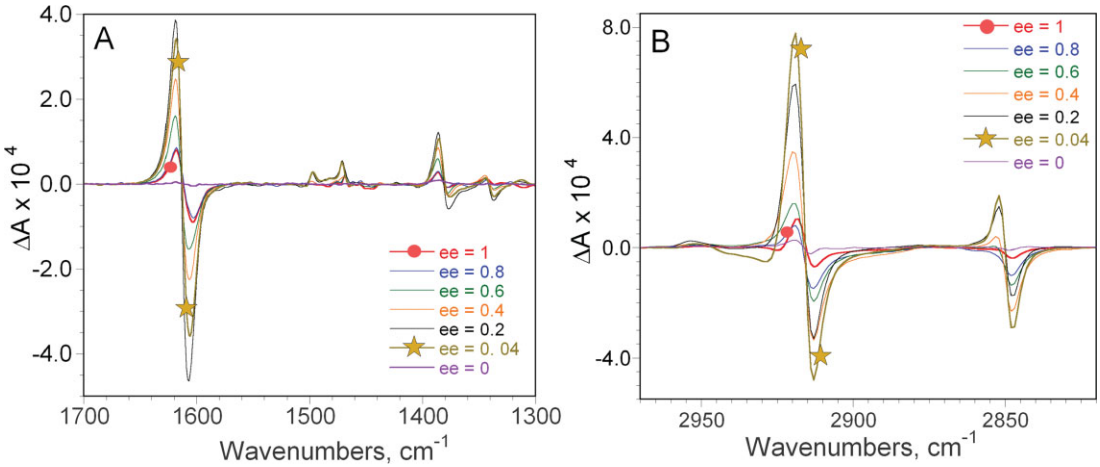

Fig. 9. VCD spectra of various mixtures of the two enantiomers of 16-2-16 tartrate recorded at room temperature at 100 mM in D_2O with a path length of 50 μm (**A**) in the 1700–1300 cm^{-1} region and (**B**) in the 3000–2800 cm^{-1} region. [Color figure can be viewed in the online issue, which is available at www.interscience.wiley.com.]

sense when the polymer is longer and presumably more folded on itself.

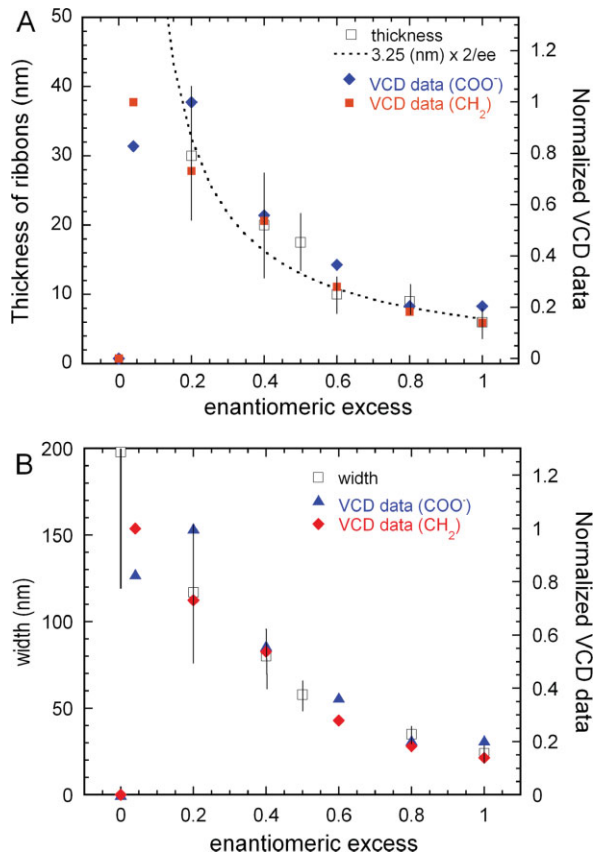

Fig. 10. (**A**) Variation of the thickness of the ribbons (left) and the normalized VCD data (right) as a function of enantiomeric excess. Using the bilayer thickness obtained from X-ray diffraction from Ref. 6 (i.e., 3.25 nm), ribbons thickness (in nm) can be calculated as 3.25 × 2/ee nm. (**B**) Variation of the width of the ribbons (left) and the normalized VCD data (right) as a function of enantiomeric excess. [Color figure can be viewed in the online issue, which is available at www.interscience.wiley.com.]

CONCLUSIONS

This study shows that important information on the molecular chirality of micellar solutions and on the supramolecular chirality of self-organized systems can be drawn from electronic and vibrational circular dichroism experiments. It has been found that tartrate salts show a strong preference for the anticonformation in micellar solutions. This conformation is independent on the solvent used and on the size and the nature of the cations (sodium, cetyl-trimethylammonium, or dimeric surfactant 12-2-12). The ECD and VCD spectra are strongly modified upon forming bilayer membranes of 16-2-16 tartrates. These spectral changes are essentially due to the chiral arrangement of the tartrate dianions and the amphiphile cations in the bilayers rather than a conformational change of the tartrate ions. Observation of VCD bands for the vibrations of cationic amphiphiles clearly demonstrates the chiral induction in the multi-bilayer structure, allowing the expression of molecular chirality at the supramolecular scale. Finally, ECD and VCD exhibit two different behaviors when 16-2-16 L-tartrate and 16-2-16 D-tartrate are mixed in various proportions. The dependence of the ECD intensity on the enantiomeric excess is correlated to the macroscopic chirality which is expressed as the inverse of the pitch period of the twisted ribbons, whereas the dependence of the VCD intensity is strongly affected by the size of the ribbons.

ACKNOWLEDGMENTS

T.B., L.D., and D.C. acknowledge computational facilities provided by the Pôle Modélisation of the Institut des Sciences Moléculaires (University Bordeaux 1).

LITERATURE CITED

1. Ihara H, Takafuji M, Sakurai T. Self-assembled nanofibers. In: Nalwa HS, editor. Encyclopedia of nanoscience and nanotechnology, Vol. 9. Stevenson Ranch, CA: American Scientific Publishers; 2004. p 473–495.
2. Brizard A, Oda R, Huc I. Chiral effects in self-assembled fibrillar networks. Top Curr Chem 2005;256:167–218.

3. Oda R, Huc I, Candau SJ. Gemini surfactants as new, low molecular weight gelators of organic solvents and water. Angew Chem Int Ed 1998;37:2689–2691.
4. Oda R, Huc I, Schmutz M, Candau SJ, Mackintosh FC. Tuning bilayer twist using chiral counterions. Nature 1999;399:566–569.
5. Berthier D, Buffeteau T, Leger JM, Oda R, Huc I. From chiral counterions to twisted membranes. J Am Chem Soc 2002;124:13486–13494.
6. Oda R, Artzner F, Laguerre M, Huc I. Molecular structure of self-assembled chiral nanoribbons and nanotubules revealed in the hydrated state. J Am Chem Soc 2008;130:14705–14712.
7. Gawronski J, Gawronska K, Skowronek P, Rychlewska U, Warzajtis B, Rychlewski J, Hoffmann M, Szarecka A. Factors affecting conformation of (R,R)-tartaric acid ester, amide and nitrile derivatives. X-ray diffraction, circular dichroism, nuclear magnetic resonance and ab initio studies. Tetrahedron 1997;53:6113–6144.
8. Salvadori P, Ciardelli F. An introduction to chiroptical techniques: basic principes, definitions and applications. In: Ciardelli F, Salvadori P, editors. Optical rotatory dispersion and circular dichroism. London: Heyden and Sons; 1973. p 3–24.
9. Berova N, Nakanishi K, Woody RW. Circular dichroism: principles and applications, 2nd ed. New York: Wiley-VCH; 2000.
10. Gottarelli G, Lena S, Masiero S, Pieraccini S, Spada GP. The use of circular dichroism spectroscopy for studying the chiral molecular self-assembly: an overview. Chirality 2008;20:471–485.
11. Nafie LA, Dukor RK, Freedman TB. Vibrational circular dichroism. In: Chalmers JM, Griffiths PR, editors. Handbook of vibrational spectroscopy. Chichester: Wiley; 2002. p 731–744.
12. Freedman TB, Cao X, Dukor RK, Nafie LA. Absolute configuration determination of chiral molecules in the solution state using vibrational circular dichroism. Chirality 2003;15:743–758.
13. Stephens PJ, Devlin FJ. Determination of the structure of chiral molecules using ab initio vibrational circular dichroism spectroscopy. Chirality 2000;12:172–179.
14. Stephens PJ, Devlin FJ, Pan JJ. The determination of the absolute configurations of chiral molecules using vibrational circular dichroism (VCD) spectroscopy. Chirality 2008;20:643–663.
15. Wang F, Polavarapu PL, Lebon F, Longhi G, Abbate S, Catellani M. Absolute configuration and conformational stability of (*S*)-(+)-3-(2-methylbutyl)thiophene and (+)-3,4-di[(*S*)-2-methylbutyl)]thiophene and their polymers. J Phys Chem A 2002;106:5918–5923.
16. Freedman TB, Cao X, Rajca A, Wang H, Nafie LA. Determination of absolute configuration in molecules with chiral axes by vibrational circular dichroism: a C_2-symmetric annelated heptathiophene and a D_2-symmetric dimer of 1,1′-binaphthyl. J Phys Chem A 2003;107:7692–7696.
17. Burgi T, Urakawa A, Behzadi B, Ernst K-H, Baiker A. The absolute configuration of heptahelicene: a VCD spectroscopy study. New J Chem 2004;28:332–334.
18. Brotin T, Cavagnat D, Dutasta JP, Buffeteau T. Vibrational circular dichroism study of optically pure cryptophane-A. J Am Chem Soc 2006;128:5533–5540.
19. Buffeteau T, Ducasse L, Poniman L, Delsuc N, Huc I. Vibrational circular dichroism and ab initio structure elucidation of an aromatic foldamer. Chem Commun 2006;2714–2716.
20. Ducasse L, Castet F, Fritsch A, Huc I, Buffeteau T. Density functional theory calculations and vibrational circular dichroism of aromatic foldamers. J Phys Chem A 2007;111:5092–5098.
21. Smulders MMJ, Buffeteau T, Cavagnat D, Wolffs M, Schenning APHJ, Meijer EW. C_3-symmetrical self-assembled structures investigated by vibrational circular dichroism. Chirality 2008;20:1016–1022.
22. Setnicka V, Urbanova M, Pataridis S, Kral V, Volka K. Sol-gel phase transition of brucine-appended porphyrin gelator: a study by vibrational circular dichroism spectroscopy. Tetrahedron Asymmetry 2002;13:2661–2666.
23. Urbanova M, Setnicka V, Devlin FJ, Stephens PJ. Determination of molecular structure in solution using vibrational circular dichroism spectroscopy: the supramolecular tetramer of *S*-2,2′-dimethylbiphenyl-6,6′-dicarboxylic acid. J Am Chem Soc 2005;127:6700–6711.
24. Setnicka V, Urbanova M, Volka K, Nampally S, Lehn J-M. Investigation of guanosine-quartet assemblies by vibrational and electronic circular dichroism spectroscopy, a novel approach for studying supramolecular entities. Chem Eur J 2006;12:8735–8743.
25. Su CN, Keiderling TA. Conformation of dimethyl tartrate in solution. Vibrational circular dichroism results. J Am Chem Soc 1980;102:511–515.
26. Polavarapu PL, Ewig CS, Chandramouly T. Conformations of tartaric acid and its esters. J Am Chem Soc 1987;109:7382–7386.
27. Buffeteau T, Ducasse L, Brizard A, Huc I, Oda R. Density functional theory calculations of vibrational absorption and circular dichroism spectra of dimethyl-L-tartrate. J Phys Chem A 2004;108:4080–4086.
28. Zhang P, Polavarapu PL. Spectroscopic investigation of the structures of dialkyl tartrates and their cyclodextrin complexes. J Phys Chem A 2007;111:858–871.
29. Abbate S, Castiglione F, Lebon F, Longhi G, Longo A, Mele A, Panzeri W, Ruggirello A, Liveri VT. Spectroscopic and structural investigation of the confinement of D- and L-dimethyl tartrate in lecithin reverse micelle. J Phys Chem B 2009;113:3024–3033.
30. Oda R, Huc I, Candau SJ. Gemini surfactants, the effect of hydrophobic chain length and dissymmetry. Chem Commun 1997;21:2105–2106.
31. Buffeteau T, Lagugne-Labarthet F, Sourisseau C. Vibrational circular dichroism in general anisotropic thin solid films: measurement and theoretical approach. Appl Spectrosc 2005;59:732–745.
32. Nafie LA, Vidrine DW. Double modulation fourier transform spectroscopy. In: Ferraro JR, Basile LJ, editors. Fourier transform infrared spectroscopy, Vol. 3. New York: Academic Press; 1982. p 83–123.
33. Kaneko N, Kaneko M, Takahashi H. Infrared and Raman spectra and vibrational assignment of some metal tartrates. Spectrochim Acta A 1984;40:33–42.
34. Holzwarth G, Chabay I. Optical activity of vibrational transitions: a coupled oscillator model. J Chem Phys 1972;57:1632–1635.
35. Tinoco I. The exciton contribution to the optical rotation of polymers. Radiat Res 1963;20:133–139.
36. Keiderling TA. Peptide and protein conformational studies with vibrational circular dichroism and related spectroscopies. In: Berova N, Nakanishi K, Woody RW, editors. Circular dichroism: principles and applications, 2nd ed. New York: Wiley-VCH; 2000. p 621–666.